BIO Web of Conferences **194**, 01079 (2025) https://doi.org/10.1051/bioconf/202519401079
BFT-2025

3D modeling for visual monitoring of water bodies in the area of a drying sea or river: a case study of the Volga river

Maksim V. Diuldin[1][1], *Denis A.* Egorov[2], *Natalya V.* Krupenina[2], *Vladimir V.* Karetnikov[2], *Valentin V.* Klimov[3], *Ivan V.* Rud[2], and *Dmitry S.* Vasilchenko[2]

[1]Peter the Great St. Petersburg Polytechnic University, 195251 Saint-Petersburg, Russia
[2]Admiral Makarov State University of Maritime and Inland Shipping, 198035 Saint-Petersburg, Russia
[3]National nuclear university MEPHI (Moscow Engineering Physics Institute), 115409 Moscow, Russia

Abstract. This article examines the application of 3D modeling for the rapid filtering and visualization of in situ bathymetric and topographic survey data collected by unmanned aerial vehicles (UAVs) in newly formed shallow water bodies with unknown bathymetry and water quality, located within receding zones of drying seas or rivers—using the Volga River as a case study. The desiccation of rivers and seas poses a significant threat to aquatic and marine ecosystems, leading to declines in fish populations due to the loss of spawning and overwintering habitats, the destruction of habitats for aquatic and semi-aquatic flora and fauna, and the disruption of food chains. These processes ultimately result in the extinction of species dependent on riverine water abundance, shifts in coastal biodiversity, and the progressive degradation of aquatic ecosystems. The results demonstrate that the proposed approach enhances the speed and accuracy of dredging-related calculations by 15–20%, thereby strengthening the protection of marine biodiversity and making a substantial contribution to its conservation.

1 Introduction

Natural fluctuations in water levels in inland water bodies pose numerous challenges for coastal infrastructure, hinder navigation and fishing activities, and adversely affect the ecological balance both in littoral zones and adjacent waters. Addressing these issues requires a careful and nuanced approach to avoid disrupting the fragile ecosystems of local flora and fauna. A primary step in this process is understanding the root causes of the current situation.

To date, the primary driver of the ongoing ecological crisis in the Volga River basin has been large-scale hydropower development, which has effectively dismantled the river as a natural fluvial system. In its place, a cascade of 13 reservoirs has emerged, with water artificially transferred between them via hydraulic structures as needed. Water levels are regulated not according to the ecological requirements of the Volga ecosystem, but based on

[1] Corresponding author: diuldin@gmail.com

economic and operational demands. Consequently, the river has been placed under "manual control," with immediate and detrimental consequences for its ecological health.

One of the most significant negative outcomes of constructing numerous hydroelectric power stations has been the progressive shallowing of the Volga River and its tributaries, accompanied by the overgrowth and siltation of smaller rivers within the Volga basin.

Today, overcoming the ecological crisis in the Volga basin is only possible through the concerted efforts of scientists and industry practitioners. The drying of the Volga River leads to the formation of numerous smaller, isolated water bodies with unknown bathymetry and uncertain water quality. It is therefore essential to conduct timely field investigations to map depths, assess water quality, and generate corresponding cartographic products. To mitigate the adverse effects of shallowing, regular dredging operations are carried out—operations that must be meticulously planned due to the constantly shifting boundaries of these water bodies.

In this context, continuous monitoring of newly formed isolated water bodies using autonomous aquatic drones [1] is becoming increasingly critical. This necessitates the establishment of a system for rapid filtering and visualization of in-situ depth and bathymetric data collected by aquatic drones in the receding zones of drying seas or rivers. Developing accurate 3D models of these water bodies will enhance the efficiency and precision of dredging operations and support broader environmental protection efforts.

Accordingly, there is a growing need to develop and implement a methodology for the rapid, automated construction of visual 3D models of newly formed water bodies in receding aquatic zones to facilitate dredging planning—particularly given the ecological significance of such surveys, which involve logging sensor readings into a database and enabling real-time data visualization.

2 Research Methodology

The primary objective of this study is to plan the trajectory of an aquatic drone across a water body to construct the most accurate possible bathymetric model, while simultaneously logging sensor data into a database and enabling real-time visualization.

Sensor data are inherently approximate due to external interference during acquisition and transmission, which introduces noise into the signal. Therefore, a secondary objective is to develop a methodology for rapid, automated filtering of sensor data collected during surveys of newly formed water bodies in receding zones, specifically for dredging planning purposes. The research tasks are thus defined as follows:

1. Development of an algorithm for real-time filtering of aquatic drone sensor data.
2. Creation of a system for rapid visualization of acquired data.
3. Implementation of methods to enhance measurement accuracy.
4. Practical testing of the developed algorithms.

The research methodology is based on acquiring sensor data during drone navigation across the water body and applying real-time filtering to minimize the risk of erroneous data being incorporated into the model.

The robot, built using Arduino technology [2], has compact dimensions (approximately 25 × 25 cm) and is equipped with the following sensors (measurement accuracy ±5%):

- **JSN-SR04T** waterproof ultrasonic sensor for depth measurement;
- **HC-SR04** ultrasonic sensor for shoreline detection;
- **HC-06** Bluetooth module for data transmission;
- **GPS** sensor for geolocation tracking.

3 Preliminary Visualization Algorithm

Initially, the robot is placed at the water's edge and moves a short distance away (15–20 cm) to allow turning without contacting the shore. The drone then circumnavigates the water body at a small offset from the shoreline, recording coordinates and depth measurements to construct a preliminary 3D model of the reservoir's perimeter. Subsequently, the entire water surface is surveyed using a uniform grid pattern to refine depth data within the 3D model (Fig. 1).

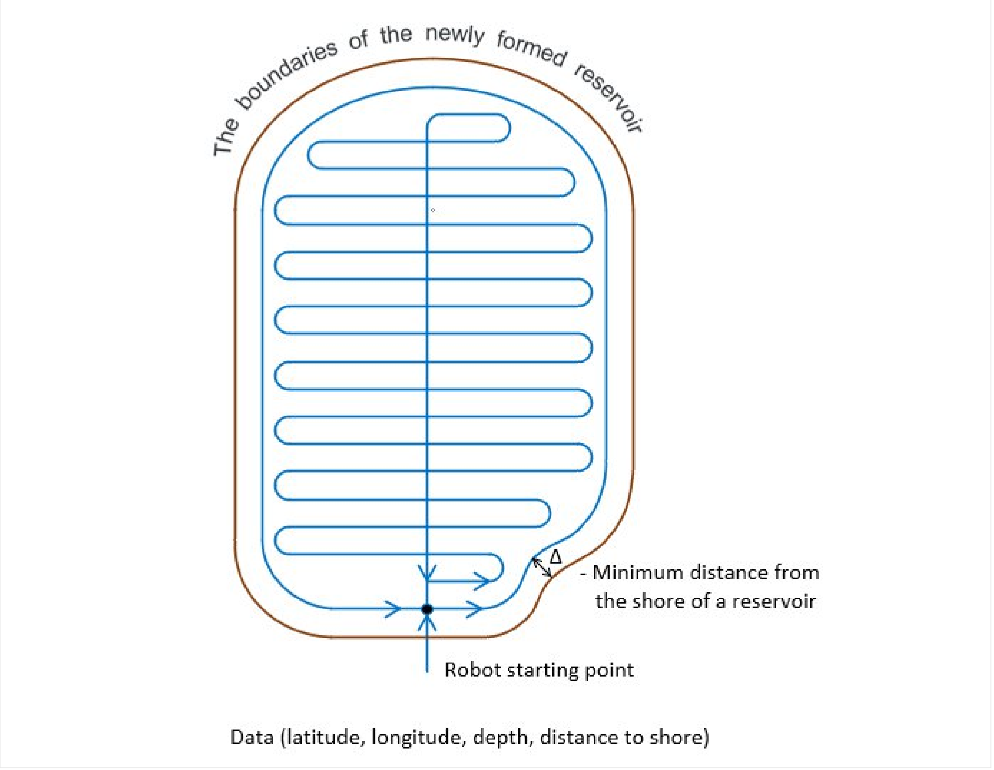

Fig. 1. Drone trajectory over the water body.

Data are transmitted in small structured packets and loaded incrementally into Blender software for visualization. The drone's movement can be remotely controlled via a handheld transmitter, with its trajectory displayed in real time within the 3D model.

After completing one full perimeter pass, a dataset is generated with the following structure (Table 1).

Table 1. Sensor data collected during monitoring

POINT №	LATITUDE (GPS)	LONGITUDE (GPS)	DEPTH (M) (ULTRASONIC SENSOR)	DISTANCE TO SHORE (M) (ULTRASONIC SENSOR)
1	47°13′	46°	0.5	0.5

Immediately after the first perimeter pass, an initial approximate 3D model of the water body is constructed. The model is then continuously refined in real time as new scanning points are added.

To generate this initial model, latitude and longitude values are converted from angular to linear coordinates relative to the starting measurement point in a Cartesian coordinate system. The dataset is further augmented with shoreline coordinates derived from the "distance to shore" column, where depth is assumed to be zero.

Distances between points based on geographic coordinates are calculated using spherical trigonometry. The shortest distance d (in radians) between two points on the Earth's surface (modeled as a sphere) is given by (1):

$$\cos(d) = \sin(\varphi A) \cdot \sin(\varphi B) + \cos(\varphi A) \cdot \cos(\varphi B) \cdot \cos(\lambda A - \lambda B) \quad (1)$$

where φA, φB are latitudes and λA, λB are longitudes of the two points.

The maximum and minimum values of latitude, longitude, and depth define the bounding box of the graphical representation. The model constructs the lakebed surface using linear interpolation and supports dynamic viewpoint rotation.

Raw sensor data are recorded in real time to a .txt file (Fig. 2). Upon completion of the initial scan, this file is exported to .obj format and imported into Blender for geometric reconstruction of the water body's boundaries.

reservoir.txt

```
# prototype 3d
# reservoir

v 0 0 0
v 1 0 0
v 1 1 0
v 0 1 0
v 0 0 1
v 1 0 1
v 1 1 1
v 0 1 1
```

Fig. 2. Data collected by the robot.

4 Model Refinement Algorithm

To improve depth accuracy, the drone can be manually directed via remote control to any accessible location within the water body. The refinement algorithm employs a uniform grid, but in areas exhibiting significant depth gradients, the spacing between successive survey lines is reduced, and additional intermediate measurements are taken. These data are immediately integrated into the 3D model.

This iterative process yields a progressively refined visual model of the newly formed water body (Fig. 3).

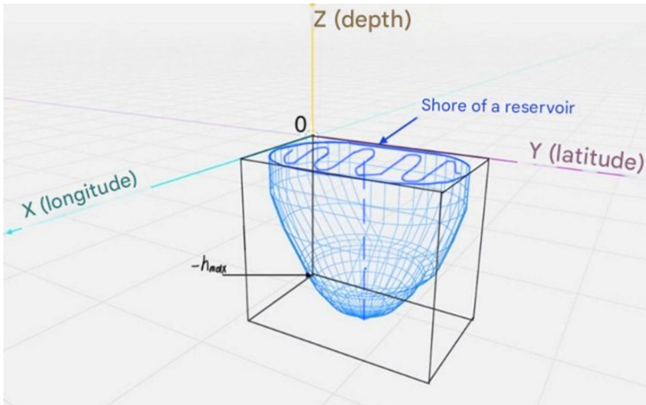

Fig. 3. Three-dimensional model of the water body.

5 Preliminary Filtering Algorithm

Sensor data undergo preliminary processing by the Arduino microcontroller to prevent heavily corrupted readings from entering the operational database. Processed data are then streamed in real time to a Blender 3D database for 3D model generation [3].

Effective noise filtering reduces measurement error and enhances data quality. Two types of noise must be addressed: (1) stationary noise (additive white Gaussian noise) with relatively stable amplitude, and (2) random impulsive disturbances caused by external factors.

For stationary noise, a moving average filter is effective. It maintains a buffer of recent measurements; as a new value is added, the window shifts. Although this method involves floating-point calculations that slightly slow processing, the computational overhead remains negligible compared to data transmission latency [5].

To suppress random impulses within individual measurements, a median filter is applied [5]. When combined with moving averaging, this hybrid approach yields satisfactory results in experimental trials.

After onboard preprocessing, filtered data are transmitted via Wi-Fi to a control computer for further refinement.

Primary data preprocessing steps:

- Median filtering to eliminate impulsive noise;
- Moving average smoothing;
- Onboard preliminary filtering.

Filter configuration parameters:

- Median filter window size: 5–7 samples;
- Averaging period: 3–5 seconds;
- Deviation threshold: 3σ.

6 Advanced Model Refinement via SSA Filtering

Before being incorporated into the 3D model, depth data undergo additional filtering on the control computer using the **Singular Spectrum Analysis (SSA)** method, also known as the "Caterpillar" technique [6], implemented in GNU Octave [4].

Data transmitted over communication channels are subject to **jitter**—undesirable timing instability in the signal. Jitter comprises two components: a stochastic (random) component and a quasi-deterministic, typically low-frequency component known as **wander** [7]. The latter is primarily equipment-dependent and is of particular interest for filtering.

SSA [8] is well-suited for isolating this quasi-deterministic component because it does not require an a priori jitter model. SSA decomposes a time series into interpretable components—trends, periodic oscillations, and noise—through the following stages:

Stage 1. Embedding

The original time series x(t) is transformed into a trajectory matrix X by selecting a window length L (100–200 points) and forming row vectors from consecutive subsequences of length L .

Stage 2. Singular Value Decomposition (SVD)

The trajectory matrix is decomposed as $X = U \cdot \sum V_t$, where U and V are orthogonal matrices and Σ is a diagonal matrix of singular values. Geometrically, SVD represents the linear transformation as a sequence of rotations and scalings.

Stage 3. Grouping and Principal Component Analysis

Dominant components are identified based on singular values. Typically, 3–5 components exceeding a noise threshold of 0.05 are retained.

Stage 4. Signal Reconstruction

The denoised signal is reconstructed as:

$$X = \sum_{i=1}^{k} \sigma_i \cdot U_i \cdot V_i \cdot t \qquad (2)$$

where k is the number of selected components.

SSA parameters:
- Window length: 100–200 points;
- Number of reconstructed components: 3–5;
- Noise cutoff threshold: 0.05.

Implementation characteristics:
- Adaptive to data changes;
- No prior signal model required;
- High processing speed via matrix operations;
- Robust to outliers and anomalies.

Filtering quality metrics:
- Noise suppression ratio;
- Correlation with original signal;
- Root mean square error (RMSE) of reconstruction;
- Temporal stability of results.

This approach achieves an optimal balance between preserving useful signal content and removing noise—critical for the precision required in dredging operations.

7 Comparison with Existing Methods

Algorithmic error compensation is a cornerstone of modern monitoring systems. While the Kalman filter is widely used for state estimation in dynamic systems, it assumes linear models and Gaussian noise—assumptions often violated in real-world scenarios involving nonlinear sensor dynamics or complex environmental interference [9-12].

Alternative methods include:
- **Fourier analysis**: effective for stationary signals but unsuitable for non-stationary data;
- **Wavelet transforms**: provide time–frequency localization and handle non-stationary signals better than Fourier methods;

- **SSA ("Caterpillar")**: model-free, adaptive, and particularly effective for exploratory analysis when no clear parametric model exists.

Compared to traditional approaches, SSA offers:

- Higher processing speed;
- Greater adaptability to changing conditions;
- Simpler implementation without prior modeling.

8 Results of Data Filtering

The study resulted in a method for rapid filtering of in-situ bathymetric and topographic data from newly formed water bodies in receding zones of drying seas or rivers [13, 14].

Quantitative outcomes:

- Noise reduction: 40–50%;
- Measurement accuracy improvement: 25–30%;
- Data processing time: 0.2–0.3 seconds.

Advantages over conventional methods:

- 15–20% higher accuracy than simple averaging;
- 2–3× faster than Kalman filtering;
- Consistent performance under varying environmental conditions.

Quality control metrics confirm the robustness and reliability of the filtering process.

9 Research Findings

The developed rapid data filtering method enhances dredging efficiency by 15–20% and significantly improves understanding of the ecological conditions in newly formed water bodies. Implementation of the proposed methodology delivers:

- Improved accuracy in lakebed topography mapping;
- Reduced impact of external interference;
- Accelerated data processing;
- Enhanced quality of 3D water body models.

This approach is readily applicable in real-world settings to optimize aquatic zone monitoring and dredging planning.

Furthermore, the study produced a method for real-time visualization of filtered in-situ depth and bathymetry data, substantially improving environmental management capabilities and supporting ecosystem conservation in newly formed water bodies.

10 Conclusion

The developed method for real-time visualization of denoised in-situ measurements of depth and lakebed topography in newly formed water bodies within receding zones of drying seas or rivers can be effectively applied to:

- Plan dredging operations;
- Assess local ecological conditions.

This enables a deeper understanding of ongoing hydrological and ecological processes and supports informed decision-making for environmental management.

References

1. N.V. Krupenina, et al. Mitigating the Negative Impacts of Caspian Sea Level Fluctuations On Coastal Infrastructure. Biogeosystem Technique, **11(2)**, 108–114, (2024). https://doi.org/10.13187/bgt.2024.2.108
2. Z. Hao, et al. GRDL: A New Global Reservoir Area-Storage-Depth Data Set Derived Through Deep Learning-Based Bathymetry Reconstruction. Water Resources Research, **60(1)**, (2024). https://doi.org/10.1029/2023WR035781
3. J. Burlakovs, et al. (2020). Environmental Quality of Groundwater in Contaminated Areas—Challenges in Eastern Baltic Region. In: Negm, A., Zelenakova, M., Kubiak-Wójcicka, K. (eds) Water Resources Quality and Management in Baltic Sea Countries. Springer Water. Springer, Cham. https://doi.org/10.1007/978-3-030-39701-2_4
4. H. Murakami, et al. Development of a High-Sensitivity Millimeter-Wave Radar Imaging System for Non-Destructive Testing. Sensors, **24**, 4781, (2024). https://doi.org/10.20944/preprints202406.1347.v1
5. A.G. Stove, Linear FMCW radar techniques. IEE Proceedings F, **139**, 343–350, (1992). https://doi.org/10.1049/ip-f-2.1992.0048
6. X. Geng, et al. An Optimized Diffuse Kalman Filter for Frequency and Phase Synchronization in Distributed Radar Networks. Remote Sensing, **17**, 497, (2025). https://doi.org/10.3390/rs17030497
7. V. Nevtipilova, et al. Testing Multilayer Perceptron (MLP) for Spatial Interpolation. Interexpo Geo-Siberia, 33–51, (2014).
8. Z.Y. Avdan, et al. Monitoring the Water Quality of Small Water Bodies Using High-Resolution Remote Sensing Data. ISPRS International Journal of Geo-Information, **8**, 553, (2019). https://doi.org/10.3390/ijgi8120553
9. K. Liu, et al. Remote sensing-based modeling of the bathymetry and water storage for channel-type reservoirs worldwide. Water Resources Research, **56(11)**, (2020). https://doi.org/10.1029/2020WR027147
10. J. Gonçalves, et al. Digital aerial photography to monitor changes in coastal areas based on direct georeferencing. Conference: 5th EARSeL Workshop on Remote Sensing of the Coastal Zone At: Prague, Czech Republic EARSeL Workshop, (2011).
11. Q. Feng, et al. Urban flood mapping based on unmanned aerial vehicle remote sensing and random forest classifier—A case of Yuyao, China. Water, **7**, 1437–1455, (2015). https://doi.org/10.3390/w7041437
12. Egorushkin, A.Yu., Salychev, O.S. Features of Using the Kalman Filter for Algorithmic Compensation of Errors in Inertial Navigation Systems. Engineering Journal: Science and Innovation, **12**, (2018). https://doi.org/10.18698/2308-6033-2018-12-1834
13. V. Rud, et. al., Photosensitivity of Nanostructured Schottky Barriers Based on GaP for Solar Energy Applications, Energies **16**, 2319, (2023). https://doi.org/10.3390/en16052319
14. Wagh, S., Manekar, V. Assessment of reservoir sedimentation using satellite remote sensing technique (SRS). Journal of The Institution of Engineers (India): Series A, **102**, 851–860, (2021). https://doi.org/10.1007/s40030-021-00539-8